Intermedin1-53 Inhibits NLRP3 Inflammasome Activation by Targeting IRE1α in Cardiac Fibrosis

Lin-Shuang Zhang
Peking University
Jin-Sheng Zhang
Peking University
Yue-Long Hou
Peking University
Wei-Wei Lu
Peking University
Xian-Qiang Ni
Peking University
Fan Lin
Peking University Third Hospital
Xiu-Ying Liu
Chinese Academy of Sciences
Xiu-Jie Wang
Chinese Academy of Sciences
Yan-Rong Yu
Peking University
Mo-Zhi Jia
Peking University
Chao-Shu Tang
Peking University
Ling Han
Beijing Fuxing Hospital
San-Bao Chai
Peking University International Hospital
Yong-Fen Qi (yongfenqi@163.com)
Peking University https://orcid.org/0000-0001-6514-0491

Research Article

Keywords: intermedin, cardiac fibrosis, NLRP3 inflammasome, ER stress, cAMP/PKA

Posted Date: November 5th, 2021

DOI: https://doi.org/10.21203/rs.3.rs-1014114/v1

Version of Record: A version of this preprint was published at Inflammation on February 17th, 2022. See the published version at https://doi.org/10.1007/s10753-022-01642-z.

Abstract

Intermedin (IMD), a paracrine/autocrine peptide, protects against cardiac fibrosis. However, the underlying mechanism remains poorly understood. Previous study reports that activation of Nucleotide-binding oligomerization domain (NOD)-like receptor family pyrin domain containing 3 (NLRP3) inflammasome contributed to cardiac fibrosis. In this study, we aimed to investigate whether IMD mitigates cardiac fibrosis by inhibiting NLRP3. Cardiac fibrosis was induced by angiotensin II (Ang II) infusion for 2 weeks in rats. Western blot, real-time PCR, histological staining, immunofluorescence assay, RNA sequencing, echocardiography and hemodynamics were used to detect the role and the mechanism of IMD in cardiac fibrosis. Ang II infusion resulted in rat cardiac fibrosis, shown as over-deposition of myocardial interstitial collagen and cardiac dysfunction. Importantly, NLRP3 activation and endoplasmic reticulum stress (ERS) was found in Ang II treated rat myocardium. Ang II infusion decreased the expression of IMD and increased the expression of the receptor system of IMD in the fibrotic rat myocardium. IMD treatment attenuated the cardiac fibrosis and improved cardiac function. In addition, IMD inhibited the upregulation of NLRP3 markers and ERS markers induced by Ang II. In vitro, IMD knockdown by small interfering RNA significantly promoted the Ang II-induced cardiac fibroblast and NLRP3 activation. Moreover, silencing of inositol requiring enzyme 1 α (IRE1α) blocked the effects of IMD inhibiting fibroblast and NLRP3 activation. Pre-incubation with PKA pathway inhibitor H89 blocked the effects of IMD on the anti-ERS, anti-NLRP3 and anti-fibrotic response. In conclusion, IMD alleviates cardiac fibrosis by inhibiting NLRP3 inflammasome activation via suppressing IRE1α and cAMP/PKA pathway.

Introduction

Cardiac fibrosis is a common response to many clinical disorders such as hypertension, vascular diseases and cardiomyopathy [1–2]. Renin-angiotensin aldosterone-system (RAAS) dysregulation, inflammation, oxidative stress, endoplasmic reticulum stress (ERS), and abnormal growth factors participate in the pathogenesis of myocardial fibrosis [3–7]. Angiotensin II (Ang II), an important member of RAAS, plays key roles in the process of cardiac fibrosis [7]. Ang II activates cardiac fibroblasts (CFs), promotes CFs transforming into myofibroblasts, increases collagen synthesis, and reduces collagen degradation [8]. Therefore, inhibiting the roles of Ang II has important clinical significance for cardiac fibrosis in patients with hypertension.

As well known, inflammation is responsible for cardiac fibrosis and cardiac hypertrophy [5, 13–16]. The NOD-like receptor (NLR) family members are central players in controlling the inflammatory response. The NLR protein family participates in multiprotein complexes, termed inflammasomes [17]. NOD-like receptor family pyrin domain containing 3 (NLRP3) inflammasome, the most fully characterized inflammasome, mediates caspase-1-dependent maturation of interleukin-1β (IL-1β) and IL-18 [17–20]. NLRP3 inflammasome activation contributes to CFs transforming into myofibroblasts and collagen deposition [19–20]. Ang II, transforming growth factor-β1 (TGF-β1) and lipopolysaccharide (LPS) can activate NLRP3 inflammasome in CFs, leading to extracellular matrix deposition [20–22]. Therefore, inhibition of NLRP3 may be a therapeutic target for alleviating myocardial fibrosis.

Many studies indicated that the crosstalk between inflammation and endoplasmic reticulum stress (ERS) plays an important role in regulation of inflammation in cardiac fibrosis. ERS inhibition may attenuate cardiac inflammation in cardiac remodeling [23–24, 28]. Several ER transmembrane sensors mediate the effects of ERS, including protein kinase receptor-like ER kinase (PERK), activating transcription factor 6 (ATF6) and inositol requiring enzyme 1α (IRE1α). In particularly, activation of IRE1α initiates inflammatory responses to promote proinflammatory cytokine signaling [45–48]. Furthermore, ERS especially IRE1α activation can initiate NLRP3 inflammasome, which provides insights into the link between ERS and chronic inflammatory diseases [52]. ERS may act as the trigger and activator of the NLRP3 inflammasome in cardiovascular diseases [17, 43, 51]. However, it is unclear whether IRE1α promotes NLRP3 activation in cardiac fibrosis.

In our previous study, ERS is inhibited by intermedin (IMD, or adrenomedullin 2), which is a paracrine/autocrine bio-active polypeptide belongs to the calcitonin/calcitonin gene-related peptide (CGRP) family. Prepro-IMD is composed of 148 amino acids, which yield IMD_{1-47}, IMD_{8-47} and IMD_{1-53} by proteolytic cleavage and amidation. IMD has extensive cardiovascular protective effects via its calcitonin receptor-like receptor (CRLR)/receptor activity modifying protein (RAMP) complexes [25–26]. Our previous research showed that endogenous IMD was significantly downregulated in response to Ang II treatment in CFs, and administration of IMD_{1-53} suppressed Ang II-induced activation of CFs and cardiomyocyte hypertrophy [27–28]. Moreover, IMD prevented myocardial ischemia injury and vascular smooth muscle cell calcification by inhibiting ERS [29–30]. IMD inhibited inflammation in hyperlipidemic, diabetic, and salt-sensitive hypertension rats [31–33]. However, whether IMD inhibits NLRP3 inflammasome activation in cardiac fibrosis is unknown.

In the present study, we investigated whether IMD inhibited Ang II-activated NLRP3 inflammasome by suppressing ERS in cardiac fibrosis.

Materials And Methods

Animals and materials

All animal care and experimental protocols complied with the Guide for the Care and Use of Laboratory Animals published by the US National Institutes of Health (NIH Publication, 8th Edition, 2011) and were approved by the Animal Care Committee of Peking University Health Science Center. Male Sprague-Dawley (SD) rats were obtained from the Animal Center, Peking University Health Science Center (Beijing). Synthetic human IMD_{1-53} and human Ang II were from Phoenix Pharmaceuticals (Belmont, CA, USA). Antibodies for collagen I and III, glucose-regulated protein 78 (GRP78), GRP94, phosphorylated IRE1α (p-IRE1α) and IRE1α, ATF6, ATF4, and spliced-X-box binding protein 1 (s-XBP-1) were from Abcam PLC (Cambridge, UK). Antibodies for glyceraldehyde-3-phosphate dehydrogenase (GAPDH), α-smooth muscle actin (α-SMA), NLRP3, IL-1β, IL-18, CRLR, RAMP1, RAMP2, RAMP3 and all secondary antibodies were from Santa Cruz Biotechnology (Santa Cruz, CA, USA). Antibodies for phosphorylated PERK (p-PERK) and PERK, phosphorylated eukaryotic translation initiation factor 2α (p-eIF2α) and eIF2α were from Cell

Signaling Technology (Danvers, MA, USA). Apoptosis-associated speck-like protein containing CARD (ASC) antibody, caspase-1 antibody, phenyl butyric acid (PBA), taurine (TAU), LPS, H89, LY294002, PD98059 and Hoechst 33342 were from Sigma (St. Louis, MO, USA). Other chemicals and reagents were of analytical grade.

Cardiac fibrosis model in rats

The rat cardiac fibrosis model was prepared according to the methods [34–36] with minor modification. Eight-week-old male SD rats (250 ± 10 g) were randomly divided into 3 groups: 1) control (Con): Only sham surgery, ended the experiment 2 weeks later; 2) Ang II: Ang II (555 ng/kg/min, dissolved in sterile saline) was infused subcutaneously via Alzet mini-osmotic pumps for 2 weeks; 3) Ang II plus IMD: IMD_{1-53} (100 ng/kg/h dissolved in sterile saline) was infused subcutaneously via Alzet mini-osmotic pumps for 2 weeks at the same time as Ang II treatment described above. All rats were given normal drinking water and normal diet. After hemodynamic measurements, all animals were killed by exsanguination and hearts were quickly collected for further analysis.

Echocardiography

At the end of the experiment, rats were anesthetized by pentobarbital sodium (40 mg/kg, i.p.). The rats underwent ultrasonography to visualize the left ventricle (LV) with a Vevo 770TM Imaging System (Visual Sonics, Toronto, Canada). The probe, which was 17.5 MHz, was placed at the sternum of rats. 2-D directional M-mode image of the LV short axis was used to analyze LV internal diameter in systole (LVID; s), LV posterior wall thickness in systole (LVPW; s), LV anterior wall thickness in systole (LVAW; s), LV volume in systole (LV Vol; s), LV internal diameter in diastole (LVID; d), LV posterior wall thickness in diastole (LVPW; d), LV anterior wall thickness in diastole (LVAW; d), LV volume in diastole (LV Vol; d). Ejection fraction (EF) and fractional shortening (FS) was quantified by above data. All echocardiographic parameter measurements represent an average of at least 5 consecutive cardiac cycles.

Hemodynamic measurements

After echocardiography, a 2.0-F micromanometer conductance catheter was placed into the right carotid artery of rats for hemodynamic measurements. Then the catheter was advanced into the LV to measure cardiac function. Data were obtained by PowerLab with the BL-420F instrument (TaiMeng, Chengdu, China).

Non-invasive tail arterial blood pressure measurement

Arterial blood pressure was measured by the BP98A Softron tail-cuff system, the measurement was repeated at 0, 4, 7, 11, 14 days. The mean of three blood values was analyzed. The time of pressure measurement was kept consistent and the temperature of rat tails was maintained at 30-33°C.

Preparation of primary neonatal CFs and Ang II treatment

Neonatal rat CFs were isolated from 1- to 2-day-old SD rats. Briefly, after being washed in Hank's balanced salt solution (HBSS), the rat myocardium was cut into pieces and digested in HBSS including

trypsin (0.05%) and collagenase (0.055%). The supernatant was collected and added to high-glucose Dulbecco's modified Eagle medium (DMEM) containing 10% fetal bovine serum (FBS). After centrifugation for 10 min at 1000 rpm, the cell suspension was filtered with a sterile stainless-steel cell cribble and plated at 37°C for 90 min to allow CFs to attach to culture dishes. Then the medium, which mostly contained cardiomyocytes, was decanted, and purified CFs were cultured in fresh DMEM containing 10% FBS. Before reagent treatment, cells were starved with serum-free medium for 24 hr. After incubation with IMD_{1-53} (1×10^{-7} mol/L) for 30 min, CFs (1×10^{5}/mL) were stimulated with Ang II (1×10^{-7} mol/L) for 24 hr as described [41–42]. CFs were stimulated with LPS (100ng/mL) for 24 hr as the positive control.

Western blot analysis

Heart tissue and rat CFs were homogenized in lysis buffer. Equal amounts of protein samples were loaded and separated on 10% SDS-PAGE, then transferred to nitrocellulose membranes for 3 hr at 4°C and 200 mA. After incubation in 5% nonfat milk for 1 hr, membranes were incubated with primary antibodies overnight at 4°C. After 3 washes for 5 min each in TBST (20 mmol/L Tris–HCl (pH 7.6), 150 mmol/L NaCl, and 0.1% Tween 20), membranes were incubated with secondary antibody (horseradish peroxidase-conjugated anti-mouse, anti-goat or anti-rabbit IgG) for 1 hr at room temperature (RT). The reaction was visualized by enhanced chemiluminescence. Protein levels were analyzed by use of NIH Image and normalized to that of GAPDH. All experiments were repeated at least 3 times.

Quantitative real-time PCR analysis

Trizol reagent was used to extract total RNA from heart tissue. An amount of 2.0 μg RNA was reverse-transcribed into cDNA. The real-time PCR (7500 Fast Real-Time PCR System, Applied Biosystems, America) was used to amplify cDNA. The amount of PCR product formed in each cycle was evaluated by Eva Green fluorescence. Relative quantification involved the $2^{-\Delta\Delta Ct}$ method, with GAPDH as a reference. The primers for real-time PCR are in **Supplement Table 3**

Immunofluorescence assay of CFs

After a rinse with phosphate buffered saline (PBS) 3 times, CFs were fixed with 4% paraformaldehyde at RT for 15 min, permeabilized with 0.1% TritonX-100 at RT for 10 min, sealed with 3% bovine serum albumin (BSA)/PBS at RT for 10 min, incubated with the antibody for α-SMA (host is rabbit) at 37°C for 1 hr, negative control was incubated with PBS at 37 ℃ for 1 hour, then anti-rabbit IgG at 37°C for 1 hr in the dark, then Hoechst 33342 (10 μg/mL, diluted in 0.5% BSA/PBS) at RT for 5 min in the dark, mounted with 50% glycerin, and observed under an immunofluorescence microscope.

Hematoxylin & eosin (H&E) staining

Hearts were excised and fixed in 4% paraformaldehyde, embedded in paraffin, cut into three 5-μm-thick sections, one of which was used as negative control, stained with hematoxylin for 15 min and with eosin for 3 min, underwent ethanol dehydration, xylene transparency, and neutral gum mounting, and observed under a microscope. 5 visual fields were randomly selected, and standardized light conditions were

always used to take photos. 50 cells were randomly selected from each visual field, and Image J was used to measure the cross-sectional area of the cardiomyocyte, and the average value was taken.

Picrosirius red staining

Hearts were excised and fixed in 4% paraformaldehyde, embedded in paraffin, cut into three 5-μm-thick sections, one of which was used as negative control, placed into 0.1% picrate Sirius-red dye solution for 1 min, then underwent ethanol dehydration, xylene transparency, and neutral gum mounting, and observed under a microscope. Image J was used to quantify the percentage of fibrotic areas in 5 randomly selected visual fields, and the average value was taken.

siRNA transfection and identification

Small interfering RNAs (siRNAs) were designed to target IMD and IRE1α in rat CFs. A scramble siRNA was used as negative control. After seeding into 6-well plates for 24 hr, CFs were cultured in serum-free medium for an additional 24 hr, then transfected with IMD, IRE1α or scramble siRNA by using transfection reagent (Lipofectamine RNAiMAX, Invitrogen).

RNA sequencing and analysis of RNA-Seq data

As described previously [37], cDNA was synthesized and purified by mRNA, which was enriched and fragmented into short fragments. Subsequently, samples were amplified by PCR, and sequenced on the Illumina HiSeq 2000. Because of the existence of poor samples, we detected the expression of gold standard marker genes of cardiac remodeling, followed by sample clustering and filtering. Then, differentially expressed genes were identified by 1.5-fold change in expression and false discovery rate (FDR) < 0.1 between 2 conditions (control vs. Ang II and Ang II vs. IMD). Gene ontology (GO) analysis was used to classify genes most likely to be associated with the development of Ang II-induced cardiac fibrosis [38–39].

Statistical analysis

Graphpad software (GraphPad Software Inc., San Diego, CA, USA) was used for analyzing data, which were expressed as mean ± SD. Comparisons of 2 groups were analyzed by Student's t test. Comparisons of more than 2 groups were analyzed by one-way ANOVA followed by Student–Newman–Keuls test. $P<0.05$ was considered significant.

Results

IMD_{1-53} inhibited NLRP3 inflammasome activation induced by Ang II in cardiac fibrosis

Firstly, we found that the expression of IMD was decreased and its receptor system was increased in the Ang II-induced cardiac fibrosis model of rats with hypertension (Fig. 1a-b). IMD_{1-53} administration

decreased collagen deposition in rat myocardial interstitial, and reduced mRNA and protein levels of collagen I and III (Fig. 1c-e) induced by Ang II compared with control. And the anti-fibrotic effects of IMD was further confirmed in CFs *in vitro*. IMD_{1-53} pre-administration decreased the levels of collagen I and III and α-SMA (Fig. 1f-g) in Ang II-treated group. Then, we investigated whether IMD had a protective effect against Ang II-treated myocardial hypertrophy and hypertension. IMD_{1-53} attenuated the cross-sectional area of cardiomyocytes treated with Ang II (Fig. 2a), decreased the markers of hypertrophy (ANP, BNP and HW/BW) induced by Ang II (Fig. 2b). Echocardiography revealed that IMD significantly improved cardiac function markers LVPWd, LVPWs, LVAWd, LVAWs, FS, LVIDd, LVIDs and E/A with Ang II+IMD versus Ang II alone (Fig. 2c and Supplement Table S1). Dynamic changes in SBP, DBP, MBP and HR in rats were monitored on days 0, 4, 7, 10 and 14 non-invasively via the tail artery. Ang II treatment increased the functional parameters of SBP, DBP and MBP time-dependently, which was reversed by IMD_{1-53} administration (Fig. 2d-2f). However, neither Ang II nor IMD_{1-53} treatment affected HR (Fig. 2g). On day 14, Hemodynamics were measured by carotid intubation invasively. SBP, DBP, MBP, LVSP, LVEDP, LV $+dp/dt_{max}$ and LV $-dp/dt_{max}$ were reduced in Ang II+IMD group as compared with Ang II alone group (Supplement Table S2). These data suggest that IMD attenuated cardiac fibrosis, hypertrophy, cardiac dysfunction and limited hypertension induced by Ang II.

Next, we further explored the mechanism of IMD protecting against myocardial fibrosis. RNA-sequencing (RNA-seq) was used to profile the changes in gene expression in rat hearts with Ang II and IMD treatment. Overall, 1017 genes were Ang II-upregulated and IMD-downregulated. In contrast, 429 genes were downregulated by Ang II and upregulated by IMD (Fig. 3a). On Gene Ontology (GO) analysis, the most statistically significantly representative term was inflammatory response, which was involved in biological process in the development of myocardial fibrosis (Fig. 3b). Moreover, 3 ERS-related genes and 100 inflammation-related genes were Ang II-upregulated and IMD-downregulated (Fig. 3c). These results suggest that IMD attenuating the Ang II-induced myocardial fibrosis was mainly related to inflammation and ERS.

To confirm the effect of IMD on inflammation, we evaluated the inflammasome generation *in vivo* and *in vitro*. *In vivo*, IMD_{1-53} treatment decreased the Ang II-induced protein levels of NLRP3, ASC, IL-1β, IL-18 and caspase-1 (Fig. 3d-e) in rat hearts. *In vitro*, IMD_{1-53} attenuated NLRP3, ASC, caspase-1, IL-18 and IL-1β protein expression that was increased by Ang II, which has the similar effect induced by LPS in CFs (Fig. 3f-g). Thus, inhibition of NLRP3 inflammasome activation may play an important role in IMD alleviating cardiac fibrosis.

IMD_{1-53} inhibited NLRP3 inflammasome via ERS mediated by the IRE1α pathway in vitro

We further explored the potential mechanism of IMD inhibiting NLRP3. One mechanism contributing to cardiac disease is by enhancing ERS, a key event in fibrosis. In this study, IMD_{1-53} treatment decreased the protein expression of ERS markers (GRP78, GRP94, ATF6, ATF4, p-PERK, p-eIF2α, IRE1α and s-XBP-1) in rat hearts (Fig. S1a-b). These effects of IMD on ERS were confirmed in Ang II treated CFs (Fig. S2a-b). It

has been reported that ERS can initiate NLRP3 activation [51]. In particular, the IRE1α pathway is activated in response to ERS, which can induce transcription of multiple cytokines and inflammatory molecules [45–48]. Therefore, we hypothesized IMD_{1-53} inhibited NLRP3 inflammasome via IRE1α pathway. We knocked down IRE1α and IMD by siRNA in CFs (Fig. 4a-b). IMD silencing further increased the Ang II-increased protein expression of NLRP3, ASC, caspase-1, IL-1β and IL-18, which was reversed by IRE1α silencing (Fig. 4c-d). Moreover, we further confirmed that IMD silencing aggravated the Ang II-evoked fibrotic response, and IRE1α silencing blocked the fibrotic response in IMD-silenced CFs (Fig. 4e-f). These data suggest that the IMD1-53 inhibited NLRP3 inflammasome via the IRE1α pathway.

IMD_{1-53} inhibited ERS, NLRP3 inflammasome activation and cardiac fibrosis via the cAMP/PKA pathway

The post-receptor signal pathways of IMD, such as cyclic adenosine monophosphate/protein kinase A (cAMP/PKA) pathway, PI3K/Akt pathway and extracellular signal-regulated kinase 1/2 (ERK1/2) pathway, are involved in its bioactive effects [27, 29–30, 49–50]. To determine the post-receptor pathway of IMD in Ang II-induced cardiac fibrosis, H89, LY294002 and PD98059 were used to block cAMP/PKA, PI3K/Akt and ERK1/2 pathways in CFs, respectively. Preincubation with H89 reversed the effect of IMD_{1-53} inhibiting Ang II-induced ERS, but LY294002 or PD98059 had no effect (Fig. 5a-b). Next, we further explored whether IMD inhibited NLRP3 inflammasome and cardiac fibrosis through cAMP/PKA pathway. We found H89 blocked the effect of IMD_{1-53} in anti-inflammation and anti-cardiac fibrosis, but LY294002 or PD98059 could not (Fig. 5c-f). These results suggest that IMD plays its biological role mainly through cAMP/PKA signaling in cardiac fibrosis.

Discussion

The major finding of this study is that IMD can protect against myocardial fibrosis induced by Ang II and the mechanisms might be involved in attenuating NLRP3 inflammasome activation by inhibiting IRE1α pathway via cAMP/PKA signaling.

Cardiac fibrosis is a common response to many clinical disorders such as vascular diseases, hypertension and cardiomyopathy [1–2]. RAAS activation plays a key role in myocardial fibrosis, and Ang II is an important member of the RAAS [8]. According to previous literatures [34–36], we established an Ang II-induced cardiac fibrosis model in rats with pressure overload, which has the similar pathogenesis of cardiac fibrosis occurring in humans with hypertension. Here, Ang II-treated rats showed significantly increased collagen deposition and expression of fibrotic biomarkers such as collagen I and III in myocardium, which indicates a fibrotic process. These were in accordance with other reports [7–8]. Then, we found a marked decrease in IMD mRNA level and upregulated mRNA and protein levels of CRLR/RAMPs in the Ang II–treated rat heart. The changes in IMD level and its receptors in the systemic imbalance and local damage-induced cardiac fibrosis suggest that endogenous IMD plays an important role in cardiac fibrosis.

Then, we investigated whether IMD has a protective effect on Ang II-treated myocardial fibrosis *in vivo*. IMD_{1-53} inhibited myocardial fibrotic biomarkers such as collagen I and III and myocardial interstitial collagen deposition in Ang II-treated rats. IMD_{1-53} also attenuated cardiomyocyte cross-sectional area, HW/BW and mRNA levels of ANP and BNP in the myocardium of rats treated with Ang II. Moreover, IMD relieves hypertension and reduces fibrosis. So we tested whether IMD acted directly on the heart. We found that IMD_{1-53} directly attenuated collagen I and III synthesis in CFs and inhibited CFs transforming into myofibroblasts *in vitro*. Hence, IMD_{1-53} conferred significant cardioprotection against Ang II-induced myocardial fibrosis and hypertrophy. Thus, IMD acts as an autocrine or paracrine modulator of cardiac fibrosis and may have a protective role in cardiac fibrosis. These were in accordance with our previous studies [27, 53–54].

Next, we investigated the protective mechanisms of IMD against myocardial fibrosis. IMD infusion significantly attenuated inflammation in the rat cardiac fibrosis, which was consistent with previous study [53, 55]. Inflammation has been identified as a critical player contributing to cardiac fibrosis and cardiac hypertrophy [5, 13–16]. NLRP3 inflammasome, a significant inflammation regulator, participates in CFs transforming into myofibroblasts and collagen deposition [17, 19–20, 44]. Other factors such as Ang II, TGF-β1 and LPS can also activate NLRP3 inflammasome in CFs, leading to extracellular matrix deposition [20–22]. In the present study, IMD_{1-53} inhibited NLRP3-inflammasome biomarkers such as NLRP3, ASC, caspase-1, IL-18 and IL-1β induced by Ang II *in vivo*, which was also confirmed in CFs *in vitro*. These results suggest that the anti-fibrotic response of IMD_{1-53} is potentially involved in its anti-NLRP3 inflammasome activation.

We further investigated the anti-inflammatory effect of IMD. Recent data have indicated that ERS can initiate NLRP3 inflammasome activation [17]. In this study, we found that NLRP3 inflammasome activation was mediated by inhibiting ERS at least in part. ERS, a cascade of pathways, named the adaptive unfolded protein response (UPR), is initiated to recover and maintain homeostasis. However, in the event of prolonged and excessive ERS, terminal UPR is initiated and results in apoptosis, inflammation, fibroblast activation, and ultimately fibrosis development [11–12]. ERS was found to aggravate cardiac hypertrophy and fibrosis in recent studies [9–10]. Our previous studies showed that IMD_{1-53} reduced myocardial ischemia injury and vascular calcification by inhibiting ERS [29–30]. In the present study, we found that IMD_{1-53} inhibited myocardial ERS, as shown by increased levels of ERS markers in Ang II treated rats and cultured CFs. Then we further investigated which specific ERS pathways mediated IMD inhibiting Ang II-activated NLRP3 inflammasome and the fibrotic response *in vitro*. The IRE1α pathway was activated in response to ERS, which induces transcription of multiple cytokines and inflammatory molecules [45–48]. Here, we used two kinds of siRNAs to knock down IMD and IRE1α mRNA expression in CFs. IRE1α silencing significantly decreased Ang II-activated NLRP3-inflammasome and the fibrotic response *in vitro*, so Ang II activated these effects via the IRE1α pathway. In addition, IMD silencing significantly increased Ang II-activated NLRP3-inflammasome and fibrotic response, which suggested that endogenous IMD had protective effects on CF inflammation and fibrosis. Moreover, IRE1α silencing significantly reversed these effects of IMD silencing on Ang II-treated CFs,

which indicates that the IRE1α pathway potentially mediated these anti-NLRP3-inflammasome and -fibrosis effects of IMD.

Next, we revealed the signaling pathway which involved in the role of IMD inhibiting NLRP3 and ERS. IMD exerts its biological effects by nonselective interaction with the CRLR/RAMP complex. Several signaling pathways are downstream of CRLR/RAMPs, such as cAMP/PKA, PI3K/Akt, and mitogen-activated protein kinase. However, in different cells, the post receptor signaling pathway activated by IMD is different. [40] In this study, we found that H89 but not LY294002 and PD98059 could block the effects of IMD on inflammation and ERS. The actions of IMD are associated with the activation of cAMP, which is the main pathway for IMD exerting its effect. The protective effects of IMD on vascular calcification, cardiomyocyte hypertrophy, apoptosis and myocardial infarction [49–50] was mediated by the activation of cAMP/PKA signaling, which supports our finding that cAMP/PKA activation might mediate roles of IMD downregulating NLRP3 and IRE1α expression.

In summary, we provided experimental evidence that the endogenous cardiovascular-protective peptide IMD could be a paracrine/autocrine factor that prevents cardiac fibrosis by inhibiting NLRP3 inflammasome via reducing ERS and activating cAMP/PKA pathway. Thus, IMD might be an effective therapeutic target for cardiac fibrosis.

Declarations

Acknowledgements

We thank Yao Song for excellent technical assistance in echocardiography. We thank Qiang Shen for technical assistance in H&E and Picrosirius Red staining.

Funding

This research was supported by the National Natural Science Foundation of China (nos. 32071113, and 31872790) and the Beijing Natural Science Foundation (nos. 7212059)

Competing interests

All authors declare that they have no conflicts of interest.

Availability of data and material

The data and material are available from the corresponding author on reasonable request.

Author contributions

Yong-Fen Qi, Chao-Shu Tang and Jin-Sheng Zhang designed the study. Lin-Shuang Zhang, Jin-Sheng Zhang, Yue-Long Hou, Wei-Wei Lu, Xian-Qiang Ni, Fan Lin and Xiu-Ying Liu performed all experiments. Lin-Shuang Zhang and Jin-Sheng Zhang also performed the data analysis and drafted the manuscript.

Yong-Fen Qi, Xiu-Jie Wang, Yan-Rong Yu, Mo-Zhi Jia, Ling Han and San-Bao Chai critically revised the manuscript. All the authors reviewed the final manuscript.

References

[1] Ma, Z.G., Yuan, Y.P., Wu, H.M., Zhang, X., & Tang, Q.Z. 2018. Cardiac fibrosis: new insights into the pathogenesis. *International Journal of Biological Sciences*, 14: 1645-1657. doi: 10.7150/ijbs.28103

[2] Kong, P., Christia, P., & Frangogiannis, N.G. 2014. The pathogenesis of cardiac fibrosis. *Cellular And Molecular Life Sciences*, 71: 549-574. doi: 10.1007/s00018-013-1349-6

[3] Zhou, B., & Tian, R. 2018. Mitochondrial dysfunction in pathophysiology of heart failure. *Journal of Clinical Investigation,* 128: 3716-3726. doi: 10.1172/JCI120849

[4] Tanjore, H., Lawson, W.E., & Blackwell, T.S. 2013. Endoplasmic reticulum stress as a pro-fibrotic stimulus. *Biochimica et Biophysica Acta*, 1832: 940-947. doi: 10.1016/j.bbadis.2012.11.011

[5] Xiao, H., Li, H., Wang, J.J., Zhang, J.S., Shen, J., An, X.B., et al. 2018. IL-18 cleavage triggers cardiac inflammation and fibrosis upon β-adrenergic insult. *European Heart Journal*, 39: 60-69. doi: 10.1093/eurheartj/ehx261.

[6] Khalil, H., Kanisicak, O., Prasad, V., Correll, R.N., Fu, X., Schips, T., Vagnozzi, R.J., et al. 2017. Fibroblast-specific TGF-β-Smad2/3 signaling underlies cardiac fibrosis. *Journal of Clinical Investigation,* 127: 3770-3783. doi: 10.1172/JCI94753.

[7] Forrester, S.J., Booz, G.W., Sigmund, C.D., Coffman, T.M., Kawai, T., Rizzo, V., et al. 2018. Angiotensin II signal transduction: An update on mechanisms of physiology and pathophysiology. *Physiological Reviews,* 98: 1627-1738. doi: 10.1152/physrev.00038.2017.

[8] Rodriguez, P., Sassi, Y., Troncone, L., Benard, L., Ishikawa, K., Gordon, R.E., et al. 2019. Deletion of delta-like 1 homologue accelerates fibroblast-myofibroblast differentiation and induces myocardial fibrosis. *European Heart Journal,* 40: 967-978. doi: 10.1093/eurheartj/ehy188.

[9] Liu, X., Kwak, D., Lu, Z., Xu, X., Fassett, J., Wang, H., et al. 2014. Endoplasmic reticulum stress sensor protein kinase R-like endoplasmic reticulum kinase (PERK) protects against pressure overload-induced heart failure and lung remodeling. *Hypertension*, 64: 738-744. doi: 10.1161/HYPERTENSIONAHA.114.03811.

[10] Lin, Y., Zhang, X., Xiao, W., Li, B., Wang, J., Jin, L., et al. 2016. Endoplasmic reticulum stress is involved in DFMO attenuating isoproterenol-induced cardiac hypertrophy in rats. *Cellular Physiology And Biochemistry*, 38: 1553-1562. doi: 10.1159/000443096.

[11] Shih, Y.C., Chen, C.L., Zhang, Y., Mellor, R.L., Kanter, E.M., Fang, Y., et al. 2018. Endoplasmic reticulum protein TXNDC5 augments myocardial fibrosis by facilitating extracellular matrix protein folding and

redox-sensitive cardiac fibroblast activation. *Circulation Research*, 122: 1052-1068. doi: 10.1161/CIRCRESAHA.117.312130.

[12] Wu, Q.Q., Xiao, Y., Yuan, Y., Ma, Z.G., Liao, H.H., Liu, C., et al. 2017. Mechanisms contributing to cardiac remodelling. *Clinical Science (London, England: 1979)*, 131: 2319-2345. doi: 10.1042/CS20171167

[13] Verma, S.K., Garikipati, V.N.S., Krishnamurthy, P., Schumacher, S.M., Grisanti, L.A., Cimini, M., et al. 2017. Interleukin-10 inhibits bone marrow fibroblast progenitor cell-mediated cardiac fibrosis in pressure-overloaded myocardium. *Circulation*, 136: 940-953. doi: 10.1161/CIRCULATIONAHA.117.027889.

[14] Song, L., Wang, L., Li, F., Yukht, A., Qin, M., Ruther, H., et al. 2017. Bone marrow-derived tenascin-C attenuates cardiac hypertrophy by controlling inflammation. *Journal of the American College of Cardiology*, 70: 1601-1615. doi: 10.1016/j.jacc.2017.07.789.

[15] Schafer, S., Viswanathan, S., Widjaja, A.A., Lim, W.W., Moreno-Moral, A., DeLaughter, D.M., et al. 2017. IL-11 is a crucial determinant of cardiovascular fibrosis. *Nature*, 552: 110-115. doi: 10.1038/nature24676.

[16] Wang, L., Zhang, Y.L., Lin, Q.Y., Liu, Y., Guan, X.M., Ma, X.L., et al. 2018. CXCL1-CXCR2 axis mediates angiotensin II-induced cardiac hypertrophy and remodelling through regulation of monocyte infiltration. *European Heart Journal*, 39: 1818-1831. doi: 10.1093/eurheartj/ehy085.

[17] Menu, P., Mayor, A., Zhou, R., Tardivel, A., Ichijo, H., Mori, K., et al. 2012. ER stress activates the NLRP3 inflammasome via an UPR-independent pathway. *Cell Death & Disease*, 3: e261. doi: 10.1038/cddis.2011.132.

[18] Agostini, L., Martinon, F., Burns, K., Mcdermott, M.F., Hawkins, P.N., & Tschopp, J. 2004. NALP3 forms an IL-1beta-processing inflammasome with increased activity in Muckle-Wells autoinflammatory disorder. *Immunity*, 20: 319-325. doi: 10.1016/s1074-7613(04)00046-9.

[19] Bracey, N.A., Duff, H.J., & Muruve, D.A. 2015. Hierarchical regulation of wound healing by NOD-like receptors in cardiovascular disease. *Antioxidants & Redox Signaling*, 22: 1176-1187. doi: 10.1089/ars.2014.6125.

[20] Bracey, N.A., Gershkovich, B., Chun, J., Vilaysane, A., Meijndert, H.C., Wright Jr, J.R., et al. 2014. Mitochondrial NLRP3 protein induces reactive oxygen species to promote Smad protein signaling and fibrosis independent from the inflammasome. *Journal Biological Chemistry,* 289: 19571-19584. doi: 10.1074/jbc.M114.550624.

[21] Zhang, B., Liu, Y., Sui, Y.B., Cai, H.Q., Liu, W.X., Zhu, M., & Yin, X.H. 2015. Cortistatin inhibits NLRP3 inflammasome activation of cardiac fibroblasts during sepsis. *Journal of Cardiac Failure*, 21: 426-433. doi: 10.1016/j.cardfail.2015.01.002.

[22] Liu, W., Zhang, X., Zhao, M., Zhang, X., Chi, J., Liu, Y., et al. 2015. Activation in M1 but not M2 macrophages contributes to cardiac remodeling after myocardial infarction in rats: a critical role of the calcium sensing receptor/NRLP3 inflammasome. *Cellular Physiology and Biochemistry,* 35: 2483-500. doi: 10.1159/000374048.

[23] Nur, B.B., Sevtap, H., Saba, K.G.S., Orhan, U., & Emine, D.Y. 2019. Hypertension-induced cardiac impairment is reversed by the inhibition of endoplasmic reticulum stress. *Journal of Pharmacy and Pharmacology*, 71: 1809-1821. doi: 10.1111/jphp.13169.

[24] Zhang, Y., Chen, W., & Wang, Y. 2020. STING is an essential regulator of heart inflammation and fibrosis in mice with pathological cardiac hypertrophy via endoplasmic reticulum (ER) stress. *Biomedicine & Pharmacotherapy*, 125: 110022. doi: 10.1016/j.biopha.2020.110022.

[25] Zhang, S.Y., Xu, M.J., & Wang, X. 2018. Adrenomedullin 2/intermedin: a putative drug candidate for treatment of cardiometabolic diseases. *British Journal of Pharmacology*, 175: 1230-1240. doi: 10.1111/bph.13814.

[26] Ni, X., Zhang, J., Tang, C., & Qi, Y. 2014. Intermedin/adrenomedullin2: an autocrine/paracrine factor in vascular homeostasis and disease. *Science China-Life Sciences*, 57: 781-789. doi: 10.1007/s11427-014-4701-7.

[27] Yang, J.H., Cai, Y., Duan, X.H., Ma, C.G., Wang, X., Tang, C.S., et al. 2009. Intermedin1-53 inhibits rat cardiac fibroblast activation induced by angiotensin II. *Regulatory Peptides*, 158: 19-25. doi: 10.1016/j.regpep.2009.05.012.

[28] Ge, C.X., Xu, M.X., Qin, Y.T., Gu, T.T., Lou, D.S., Li, Q., et al. 2019. Endoplasmic reticulum stress-induced iRhom2 up-regulation promotes macrophage-regulated cardiac inflammation and lipid deposition in high fat diet (HFD)-challenged mice: Intervention of fisetin and metformin. *Free Radical Biology and Medicine*, 141: 67-83. doi: 10.1016/j.freeradbiomed.2019.05.031.

[29] Teng, X., Song, J., Zhang, G., Cai, Y., Yuan, F., Du, J., et al. 2011. Inhibition of endoplasmic reticulum stress by intermedin(1-53) protects against myocardial injury through a PI3 kinase-Akt signaling pathway. *Journal of molecular medicine (Berlin, Germany)*, 89: 1195-1205. doi: 10.1007/s00109-011-0808-5.

[30] Chang, J.R., Duan, X.H., Zhang, B.H., Teng, X., Zhou, Y.B., Liu, Y., et al. 2013. Intermedin1-53 attenuates vascular smooth muscle cell calcification by inhibiting endoplasmic reticulum stress via cyclic adenosine monophosphate/protein kinase A pathway. *Experimental biology and medicine (Maywood, N.J.)*, 238:1136-1146. doi: 10.1177/1535370213502619.

[31] Li, H., Bian, Y., Zhang, N., Guo, J., Wang, C., Lau, W.B., & Xiao, C. 2013. Intermedin protects against myocardial ischemia-reperfusion injury in diabetic rats. *Cardiovascular Diabetology,* 12: 91. doi: 10.1186/1475-2840-12-91.

[32] Yang, S.M., Liu, J., & Li, C.X. 2014. Intermedin protects against myocardial ischemia-reperfusion injury in hyperlipidemia rats. *Genetics and Molecular Research*, 13: 8309-8319. doi: 10.4238/2014.October.20.7.

[33] Li, Y., Zhang, H., Jiang, C., Xu, M., Pang, Y., Feng, J., et al. 2013. Hyperhomocysteinemia promote insulin resistance by inducing endoplasmic reticulum stress in adipose tissue. *Journal of Biological Chemistry*, 288: 9583-9592. doi: 10.1074/jbc.M112.431627. Epub 2013 Feb 17.

[34] Moilanen, A.M., Rysä, J., Mustonen, E., Serpi, R., Aro, J., Tokola, H., et al. 2011. Intramyocardial BNP gene delivery improves cardiac function through distinct context-dependent mechanisms. *Circulation Heart Failure*, 4: 483-495. doi: 10.1161/CIRCHEARTFAILURE.110.958033.

[35] Serpi, R., Tolonen, A.M., Huusko, J., Rysä, J., Tenhunen, O., Ylä-Herttuala, S., et al. 2011. Vascular endothelial growth factor-B gene transfer prevents angiotensin II-induced diastolic dysfunction via proliferation and capillary dilatation in rats. *Cardiovascular Resesrch,* 89: 204-213. doi: 10.1093/cvr/cvq267. .

[36] Skoumal, R., Tóth, M., Serpi, R., Rysä, J., Leskinen, H., Ulvila, J., et al. 2011. Parthenolide inhibits STAT3 signaling and attenuates angiotensin II-induced left ventricular hypertrophy via modulation of fibroblast activity. *Journal of Molecular Cell Cardiology*, 50: 634-641. doi: 10.1016/j.yjmcc.2011.01.001

[37] Chang, J.R., Guo, J., Wang, Y., Hou, Y.L., Lu, W.W., Zhang, J.S., et al. 2016. Intermedin1-53 attenuates vascular calcification in rats with chronic kidney disease by upregulation of α-Klotho. *Kidney International,* 89: 586-600. doi: 10.1016/j.kint.2015.12.029.

[38] Li, T.T., Li, X.Y., Jia, L.X., Zhang, J., Zhang, W.M., Li, Y.L., et al. 2016. Whole Transcriptome Analysis of Hypertension induced cardiac injury using deep sequencing. *Cellular Physiology And Biochemistry*, 38: 670-682. doi: 10.1159/000438659.

[39] Trapnell, C., Roberts, A., Goff, L., Pertea, G., Kim, D., Kelley, D.R., et al. 2012. Differential gene and transcript expression analysis of RNA-seq experiments with TopHat and Cufflinks. *Nature Protocol*, 7: 562-578. doi: 10.1038/nprot.2012.016.

[40] Lu, W.W., Jia, L.X., Ni, X.Q., Zhao, L., Chang, J.R., Zhang, J.S., et al. 2016. Intermedin1-53 attenuates abdominal aortic aneurysm by inhibiting oxidative stress. *Arteriosclerosis, Thrombosis, and Vascular Biology,* 36: 2176-2190. doi: 10.1161/ATVBAHA.116.307825.

[41] Zhang, J., Lang, Y., Guo, L., Pei, Y., Hao, S., Liang, Z., et al. 2018. MicroRNA-323a-3p promotes pressure overload-induced cardiac fibrosis by targeting TIMP3. *Cellular Physiology & Biochemistry*, 50: 2176-2187. doi: 10.1159/000495059.

[42] Song, Q., Liu, L., Yu, J., Zhang, J., Xu, M., Sun, L., et al. 2017. Dihydromyricetin attenuated Ang II induced cardiac fibroblasts proliferation related to inhibitory of oxidative stress. *European Journal of*

Pharmacology, 807: 159-167. doi: 10.1016/j.ejphar.2017.04.014.

[43] Wu, Q., Wang, Q., Guo, Z., Shang, Y., Zhang, L., & Gong, S. 2014. Nuclear factor-κB as a link between endoplasmic reticulum stress and inflammation during cardiomyocyte hypoxia/reoxygenation. *Cell Biology International,* 38: 881-887. doi: 10.1002/cbin.10272.

[44] Li, F., Zhang, H., Yang, L., Yong, H., Qin, Q., Tan, M., et al. 2018. NLRP3 deficiency accelerates pressure overload-induced cardiac remodeling via increased TLR4 expression. *Journal of Molecular Medicine (Berlin, Germany)*, 96: 1189-1202. doi: 10.1007/s00109-018-1691-0.

[45] Bujisic, B., & Martinon, F. 2017. IRE1 gives weight to obesity-associated inflammation. *Nature Immunology*, 18: 479-480. doi: 10.1038/ni.3725.

[46] Keestra-Gounder, A.M., Byndloss, M.X., Seyffert, N., Young, B.M., Chávez-Arroyo, A., Tsai, A.Y., et al. 2016. NOD1 and NOD2 signalling links ER stress with inflammation. *Nature*, 532: 394-397. doi: 10.1038/nature17631.

[47] Ribeiro, C.M., & Lubamba, B.A. 2017. Role of IRE1α/XBP-1 in cystic fibrosis airway inflammation. *International Journal of Molecular Sciences,* 18: 118. doi: 10.3390/ijms18010118.

[48] Yin, J., Gu, L., Wang, Y., Fan, N., Ma, Y., & Peng, Y. 2015. Rapamycin improves palmitate-induced ER stress/NF κ B pathways associated with stimulating autophagy in adipocytes. *Mediators of Inflammation,* 2015: 272313. doi: 10.1155/2015/272313.

[49] Chen, H., Wang, X., Tong, M., Wu, D., Wu, S., Chen, J., et al. 2013. Intermedin suppresses pressure overload cardiac hypertrophy through activation of autophagy. *PLoS One*, 8: e64757. doi: 10.1371/journal.pone.0064757.

[50] Wei, P., Yang, X.J., Fu, Q., Han, B., Ling, L., Bai, J., et al. 2015. Intermedin attenuates myocardial infarction through activation of autophagy in a rat model of ischemic heart failure via both cAMP and MAPK/ERK1/2 pathways. *International Journal of Clinical Experimental Pathology*, 8: 9836-9844. eCollection 2015.

[51] Ji, T., Han, Y., Yang, W., Xu, B., Sun, M., Jiang, S., et al. 2021. Endoplasmic reticulum stress and NLRP3 inflammasome: Crosstalk in cardiovascular and metabolic disorders. *Journal of Cellular Physiology*. 41: 272-277. doi: doi: 10.1097/WNO.0000000000001267.

[52] Ke, R.,Wang, Y., Hong, S., & Xiao, L. 2020. Endoplasmic reticulum stress related factor IRE1α regulates TXNIP/NLRP3-mediated pyroptosis in diabetic nephropathy. *Experimental Cell Research*, 396: 112293. doi: 10.1016/j.yexcr.2020.112293

[53] Zhang, J.S., Hou, Y.L., Lu, W.W., Ni, X.Q., Lin, F., Yu, Y.R., et al. 2016. Intermedin 1-53 protects against myocardial fibrosis by inhibiting endoplasmic reticulum stress and inflammation induced by

homocysteine in apolipoprotein E-deficient mice. *Journal of Atherosclerosis Thrombosis*, 23: 1294-1306. doi: 10.5551/jat.34082.

[54] Zhang, L.S., Liu, Y., Chen, Y., Ren, J.L., Zhang, Y.R., Yu, Y.R., et al. 2020. Intermedin alleviates pathological cardiac remodeling by upregulating klotho. *Pharmacological Research*, 159: 104926. doi: 10.1016/j.phrs.2020.104926.

[55] Wu, D., Shi, L., Li, P., Ni, X., Zhang, J., Zhu, Q., Qi, Y., et al. 2018. Intermedin 1-53 protects cardiac fibroblasts by inhibiting NLRP3 inflammasome activation during sepsis. *Inflammation*, 41: 505-514. doi: 10.1007/s10753-017-0706-2.

Figures

FIGURE 1

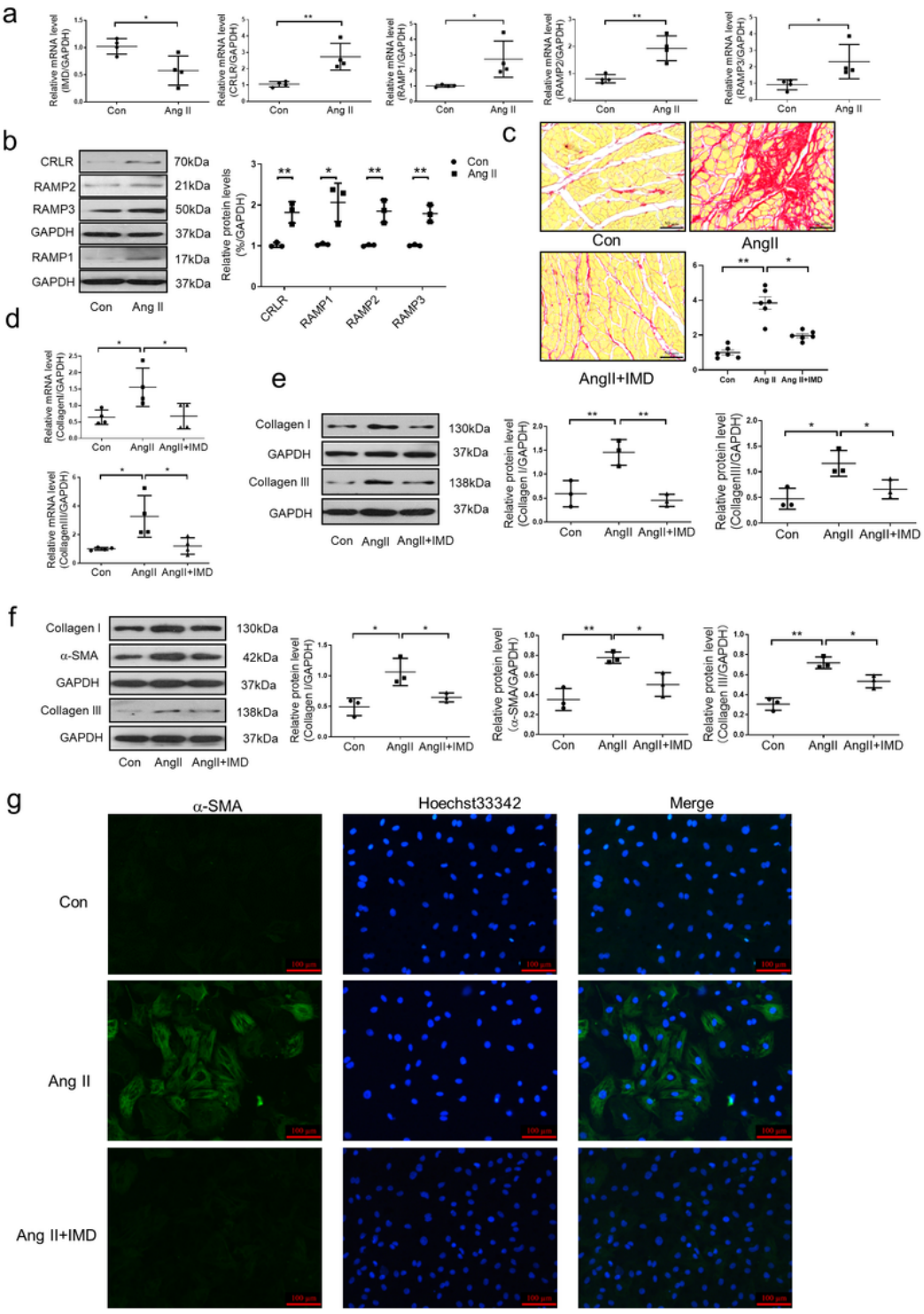

Figure 1

IMD1-53 inhibited myocardial fibrosis and hypertrophy. (a) Quantitative real-time PCR analysis of mRNA levels of IMD, calcitonin receptor-like receptor (CRLR), receptor activity modifying protein (RAMP) 1, RAMP2 and RAMP3 in rat myocardium. Results are relative to GAPDH. Data are mean ± SD (n =4 in each group), *P<0.05, **P□0.01. (b) Western blot analysis of protein levels of CRLR, RAMP1, RAMP2 and RAMP3 in rat myocardium. GAPDH is a control for protein loading. Data are mean ± SD (n =3 in each

group), *P<0.05, **P0.01. (c) Picrosirius red staining of myocardial interstitial collagen deposition in rat. The bar represents 50 μm. Data are mean ± SD (n =6 in each group), *P<0.05, **P0.01. (d) Quantitative real-time PCR analysis of mRNA levels of collagen I and III in rat myocardium. Results are relative to GAPDH. Data are mean ± SD (n =4 in each group), *P<0.05, **P0.01. (e) Western blot analysis of protein levels of (e) collagen I and III in rat myocardium and (f) collagen I and III, α-smooth muscle actin (α-SMA) in rat cardiac fibroblasts (CFs). GAPDH was a control for protein loading. Data are mean ± SD (n =3 in each group), *P<0.05, **P0.01. (g) Immunofluorescence assay of myofibroblasts differentiated from CFs stained with α-SMA antibody and Hoechst 33342 and treated with Con, Ang II, Ang II+IMD. The bar represents 100 μm.

FIGURE 2

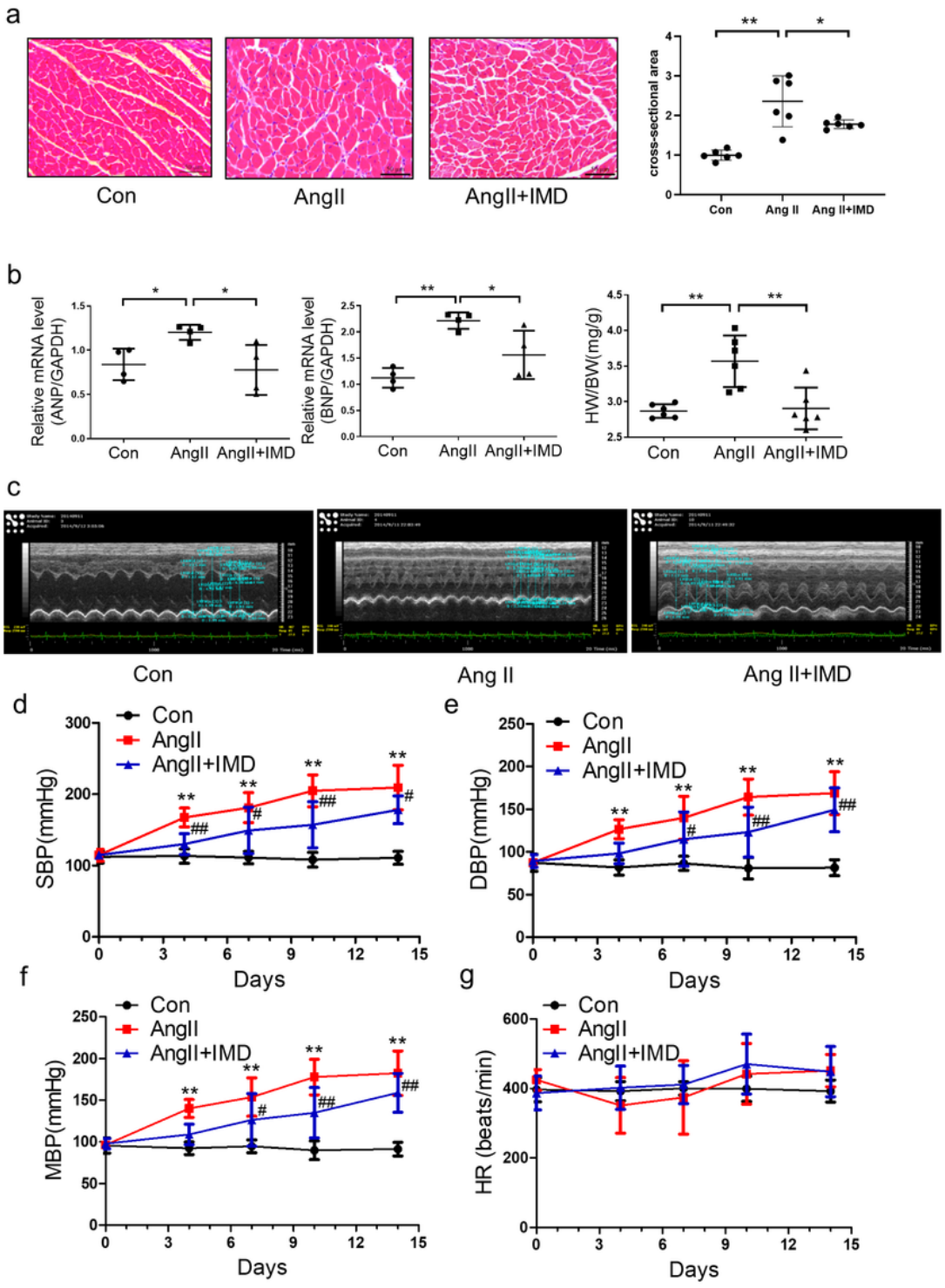

Figure 2

IMD1-53 inhibited myocardial hypertrophy and hypertension induced by Ang II in vivo. (a) Hematoxylin-eosin staining of cardiomyocyte cross-sectional area in rats. The bar represents 50 μm. Data are mean ± SD (n =6 in each group), *P<0.05, **P□0.01. (b) Quantitative real-time PCR analysis of mRNA levels of atrial natriuretic peptide (ANP) and brain natriuretic peptide (BNP) in rat myocardium. Results are relative to GAPDH. Data are mean ± SD (n =4 in each group), *P<0.05, **P□0.01. Ratio of heart weight to body

weight (HW/BW) in rats. Data are mean ± SD (n =6 in each group), *P<0.05, **P0.01. (c) Echocardiographic parameters of rats. (d) systolic blood pressure (SBP), (e) diastolic blood pressure (DBP), (f) mean blood pressure (MBP), and (g) heart rate (HR). Data are mean ± SD (n =6 in each group), *P<0.05, **P0.01.

FIGURE 3

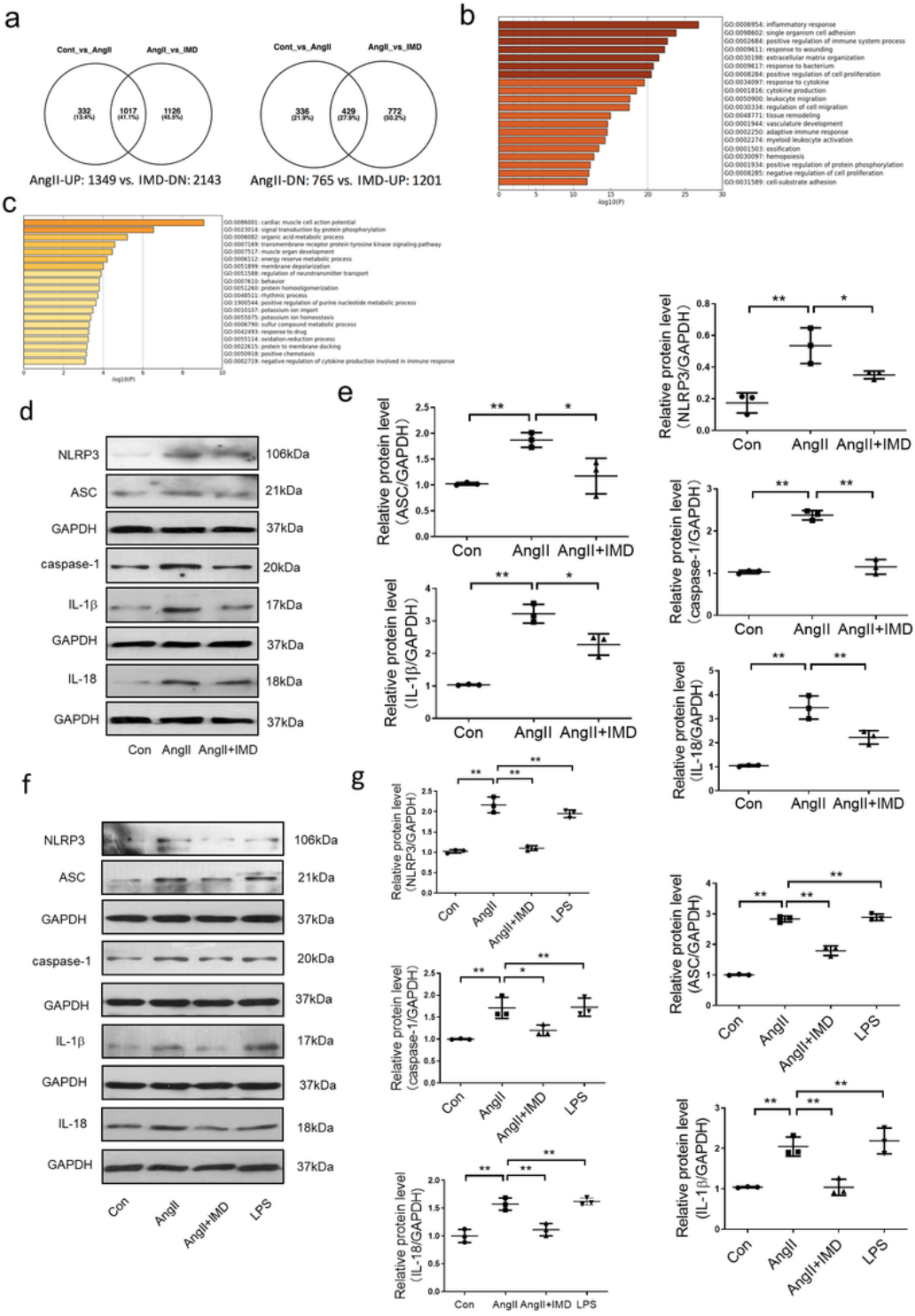

Figure 3

IMD1-53 attenuated NLRP3 inflammasome activation induced by AngII in vivo and in vitro. (a) Left, differentially expressed genes upregulated by Ang II and downregulated by IMD. Right, differentially expressed genes downregulated by Ang II and upregulated by IMD. The left circle indicates Ang II vs control, the right circle indicates Ang II vs IMD. Gene Ontology analysis of genes involved in biological processes with (b) Ang II upregulation and IMD downregulation and (c) AngII downregulation and IMD upregulation. Western blot analysis of protein levels of (d-e) NLRP3, apoptosis-associated speck-like protein containing CARD (ASC), caspase-1, interleukin-1β (IL-1β) and IL-18 in rat myocardium in vivo and (f-g) NLRP3, ASC, caspase-1, IL-1β and IL-18 in CFs in vitro. GAPDH was a control for protein loading. Data are mean ± SD (n =3 in each group), *P<0.05, **P□0.01.

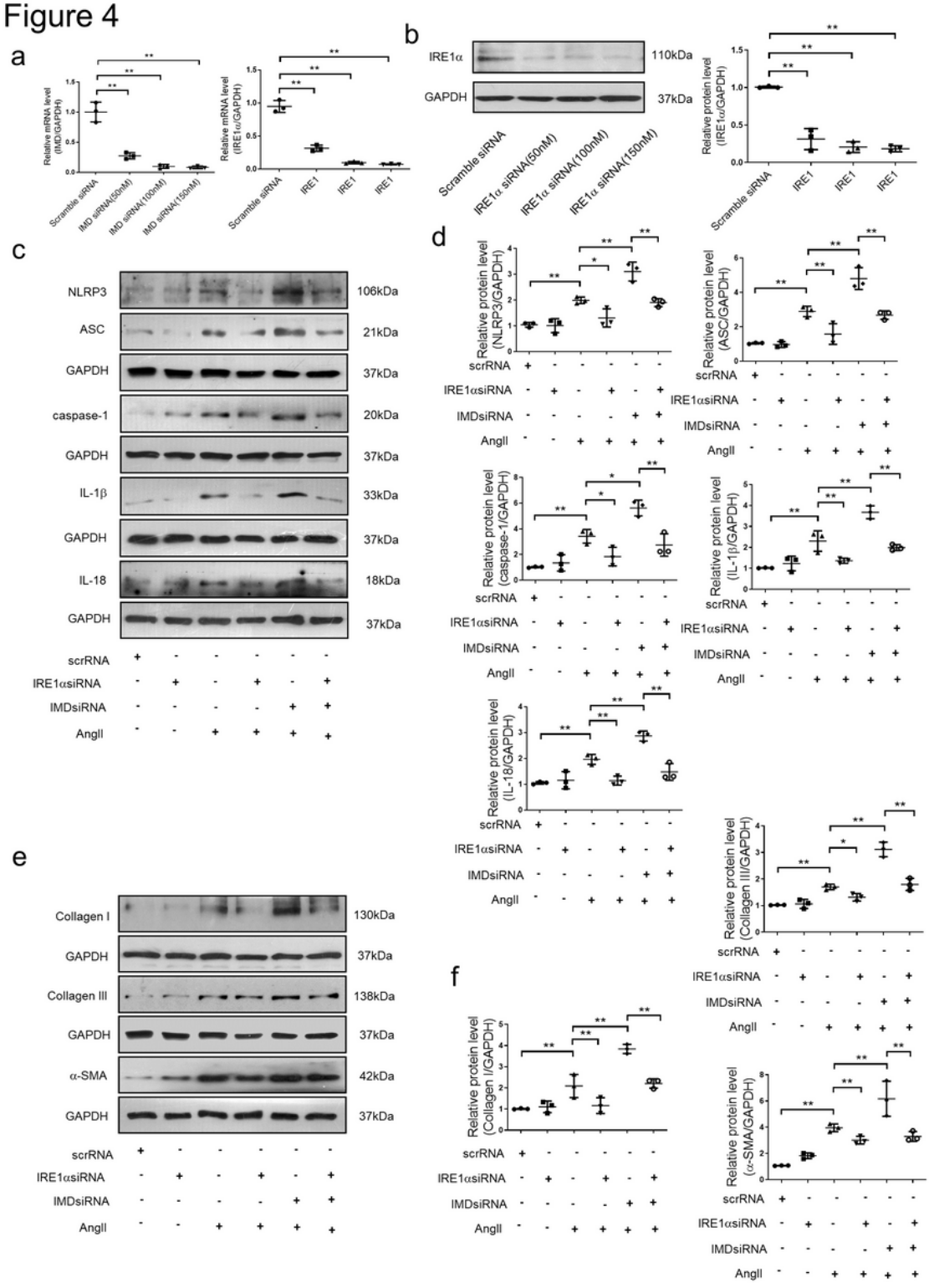

Figure 4

IMD inhibited Ang II-activated NLRP3 inflammasome and fibrotic response via IREα pathway in vitro. (a) Quantitative real-time PCR analysis of mRNA levels of IMD and IRE1α in CFs. (b-f), Western blot analysis of protein levels of IRE1α, NLRP3, ASC, caspase-1, IL-1β, IL-18, collagen I, collagen III and α-SMA in CFs. GAPDH was a control for protein loading. Results are relative to GAPDH. Data are mean ± SD (n =3 in each group), *P<0.05, **P□0.01.

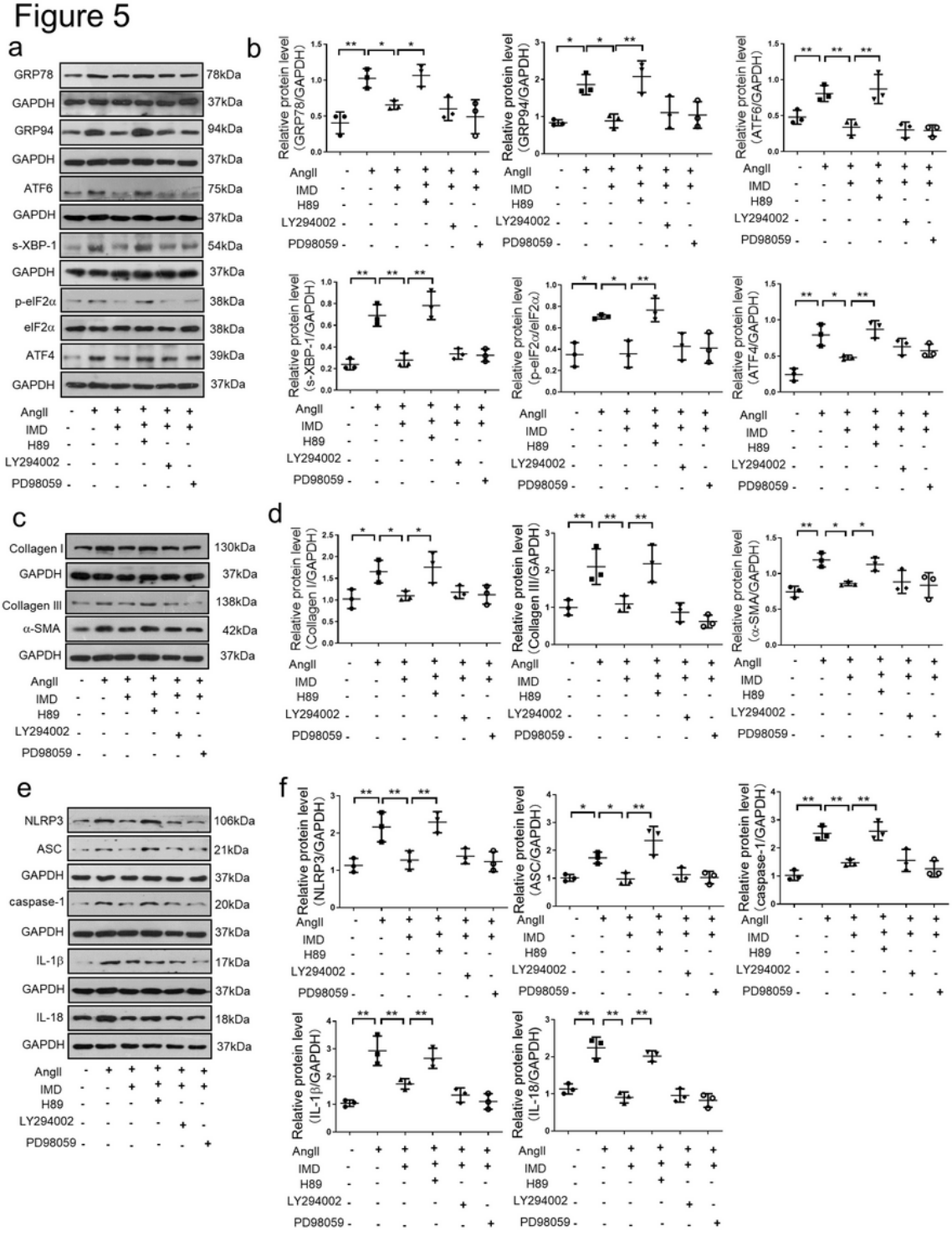

Figure 5

IMD1-53 inhibited NLRP3 inflammasome via cAMP/PKA pathway. (a-f) Western blot analysis of protein levels of collagen I, collagen III, α-SMA, GRP78, GRP94, ATF6, ATF4, p-eIF2α, s-XBP-1, NLRP3, ASC, caspase-1, IL-1β and IL-18 in CFs treated with H89, LY294002 or PD98059 to block cAMP/PKA, PI3K/Akt and ERK1/2 pathways. GAPDH was a control for protein loading. Data are mean ± SD (n =3 in each group), *P<0.05, **P□0.01.

Supplementary Files

This is a list of supplementary files associated with this preprint. Click to download.

- Supplementary.pdf